Excerpt from the Proceedings of the 2011 COMSOL Conference in Boston

Multiphysics Modeling of Electro-Optic Devices

James E. Toney
SRICO, Inc.
2724 Sawbury Boulevard, Columbus, OH 43235, jtoney@srico.com

Abstract: Designers of electro-optic modulators and related devices often use separate tools to study the optical and electrical portions of the device. The flexibility of Comsol Multiphysics makes it possible to construct unified models of EO phenomena including realistic waveguide profiles and anisotropic material properties. We demonstrate the use of the RF Module to compute both RF and optical waveguide modes and calculate the velocity mismatch and overlap efficiency between them. Realistic index profiles for diffused waveguides are computed using the Transport of Diluted Species physics mode with anisotropic diffusion coefficients.

Keywords: Electro-Optics, RF Module, Paraxial Waves, Waveguide Modes

1. Introduction

High-speed electro-optic modulator design requires detailed analysis of the interaction between RF and optical waves. The efficiency of that interaction determines the crucial operating parameters of the modulator: bandwidth and operating voltage.

Multiphysics modeling with Comsol enables direct calculation of the velocity mismatch and overlap of the RF and optical fields without overly simplified assumptions. Finite conductivities and anisotropic dielectric constants can be incorporated easily. Most of the critical parameters for high-speed modulator performance – half-wave voltage (V_π), characteristic impedance and velocity-matching bandwidth – can be determined from eigenmode computations alone.

In principle, combined RF and paraxial optical propagation models can also be constructed, for example to compute the effect of electrode loss on V_π or to model quasi-phase-matched structures. However for realistic device sizes, such simulations are too computationally intensive for 3-dimensional models to be practical with current desk-top computer resources. We illustrate the construction of a combined RF-optical propagation model through a simplified, 2-dimensional example.

2. High-Speed Electro-Optic Modulator Design Considerations

This paper focuses on waveguide-based intensity modulators for operation at microwave frequencies. The critical issues in high-speed modulator design include:

1. *Velocity matching between the RF and optical waves*. If the effective indices of the optical and RF waveguide modes are not equal, the phase between the two waves varies along the propagation direction, reducing the electro-optic efficiency. The result is a limitation of the high-frequency bandwidth that is inversely proportional to the interaction length and the effective index mismatch.[1]
2. *Half-wave voltage (V_π).* The efficiency of a modulator is characterized by the voltage that must be applied to produce a π phase difference at the output, which ideally corresponds to the transition from complete transmission to complete extinction in an intensity modulator.
3. *Electrode loss.* RF transmission loss can be caused by the finite conductivity of the metal, dielectric absorption in the substrate and radiative losses in the guided mode. The effect is to increase V_π, especially at higher frequencies.

2.1 RF Electrode Characteristics

One type of electrode structure that is often used in high-speed electro-optic intensity modulators is the coplanar waveguide in which there is a center electrode with ground conductors on each side. An illustration of this structure is shown in Figure 1. The optical waveguides, typically in a Mach-Zehnder configuration, are situated beneath the gaps between electrodes. Often there is a dielectric buffer layer between the electrodes and the substrate to reduce optical loss. An advantage of this structure is its bi-polar operation. Since the electric field lines radiate outward from the

center conductor, the two waveguides experience opposite electric field polarities, and therefore opposite electro-optic effects. The result is a reduction of V_π by a factor of 2.

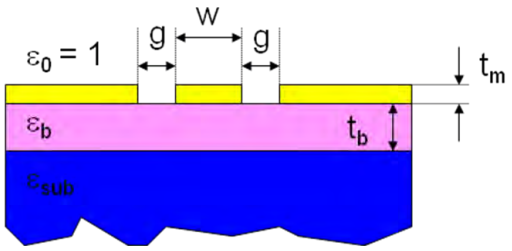

Figure 1. Illustration of coplanar waveguide electrode structure

The main parameters that are adjusted to produce the desired electrode characteristics (impedance, effective index and loss) are the center electrode width, w, the inter-electrode gap, g, and the metal and buffer thicknesses, t_m and t_b, respectively.

2.2 Diffused Optical Waveguide

In lithium niobate ($LiNbO_3$), the most widely used EO modulator material, channel waveguides are fabricated primarily by diffusion of dopants, typically either titanium or protons. Analytic approximations for the resulting index profile are commonly used in calculation of the waveguide modes. In Comsol Multiphysics, the diffusion process can be simulated directly, which enables the inclusion of anisotropic diffusion coefficients, as is known to be the case for $LiNbO_3$.[2] The relationship between dopant concentration and refractive index, which is not necessarily linear[2], can then be specified in the material or domain properties of the model. In this way, the properties of the optical waveguides as a function of fabrication conditions can be studied systematically.

2.3 Electro-Optic Interaction, V_π and Velocity-Matching Bandwidth

The basis of EO modulation is the fact that, in certain materials, the refractive index varies with an applied electric field. The linear EO effect is, strictly speaking, a special case of $\chi^{(2)}$ nonlinearity[3], but it is described through a separate tensor, r_{ij}. A complete treatment of the EO effect, accounting for all electric field components, requires diagonalization of the inverse-permittivity tensor to find a new set of principal axes, and if the E-field is non-uniform, this procedure must be carried out *at each field point*. This procedure could in principle be done via scripting in Matlab. Fortunately, for $LiNbO_3$ and related materials there is no change in the principal axes when the field is applied along the optic axis, which is also the case that gives the strongest EO effect. In most cases, it is therefore sufficient to calculate the perturbation of the refractive index by the equation[4]:

$$\Delta n_{o/e} = -\tfrac{1}{2}\, n_{o/e}^3 r_{i3}\, E_z \qquad (1)$$

where i=3, $n=n_e$ for light polarized parallel to the optic axis, and i=1, $n=n_o$ for light polarized in the plane normal to the optic axis. For the CPW geometry of Figure 1, the optic axis must be horizontal; i.e. an "x-cut" crystal is used.

3. RF and Optical Guided Mode Model

The model includes two instances of the Electromagnetic Waves physics mode, one defined for RF frequencies and one for optical frequencies. Figure 2 shows the 2D geometry for computation of RF and optical modes. In the RF mode calculation, the electrodes are defined as solid metal (gold) rather than as hollow, perfect conductors. The boundary outlined in red is a perfect electric conductor that represents the ground plane, and the lower boundary is defined as a perfect magnetic conductor (i.e. symmetry boundary). The lithium niobate substrate is treated as an anisotropic dielectric with relative permittivity of [44, 44, 28] and an isotropic loss tangent of 0.006.[5] The air and buffer layers are treated as isotropic, lossless dielectrics with ε_r=1 and 3.8, respectively.

The geometric parameters used for this example are those of a typical bulk LN, high-speed modulator, specifically w=8 μm, g=28 μm, t_m=30 μm and t_b=1 μm. The angle of the electrode side walls can be specified to match the fabrication process. In this example we use a side wall angle of 84° (i.e. 6° off of vertical).

Due to the truncation of the field at the perfectly conducting boundary, the precise solution will depend on the size of the domain. The air and substrate spaces should be made

large enough to produce adequate precision in the effective index computation, keeping in mind that the material parameters may only be known to two significant figures.

In the optical mode calculation, the electrodes are treated as hollow, perfect conductors, and the outer domain edges are treated as perfect magnetic conductors. The air and buffer layers have isotropic indices of refraction of 1 and 1.45, respectively. The lithium niobate substrate has an anisotropic index of refraction given by [n_o, n_o, $n_e+n_d+n_{EO}$] where n_o and n_e are the ordinary and extraordinary refractive indices, n_d is the contribution from the diffused waveguide and n_{EO} is the electro-optic perturbation, given by equation (1) based on the computed RF field. We are assuming waveguides fabricated by annealed proton exchange (APE), which has no effect on n_o.

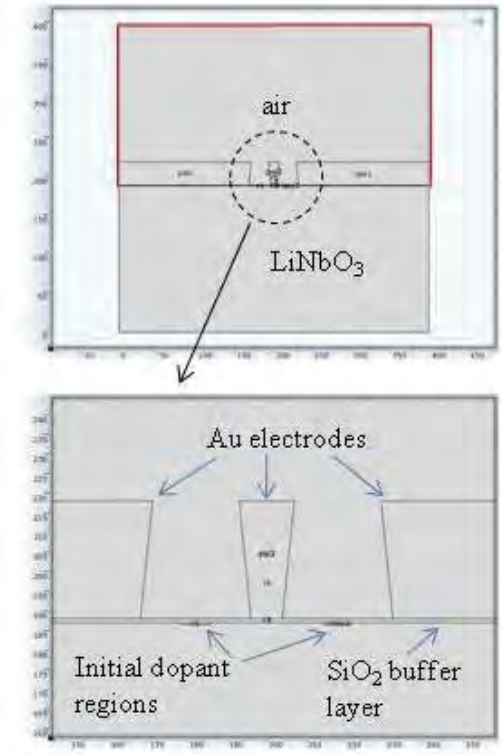

Figure 2. Geometry for 2D RF and optical mode computation

n_d is determined by simulating the diffusion process using a time-dependent Transport of Dilute Species model in Comsol, then relating the index change to the concentration through published relationships. The small rectangles at the buffer-substrate interface represent the initial regions on non-zero concentration.

3.1 RF Mode Solution, Impedance and Loss

Figure 3 shows the horizontal component of the computed field at a frequency of 10 GHz. The displacement field, Dx, is displayed rather than the electric field, since the latter is greatly reduced in the substrate due to the high relative permittivity of lithium niobate.

Once the complex effective index (n_{eff}) of the RF mode is computed vs. frequency, the loss coefficient is calculated as

$$\alpha = -2\,\pi\, f\, \mathrm{Im}(n_{eff})/c \qquad (2)$$

The real effective index and loss coefficient vs. frequency are plotted in Figure 3.

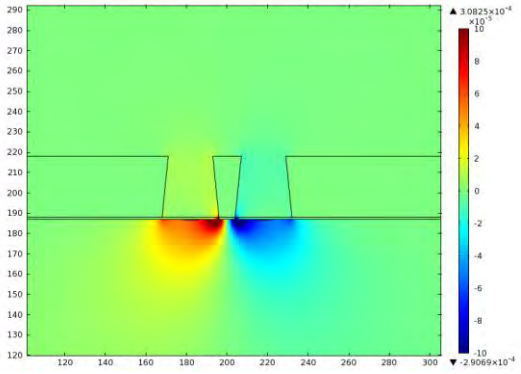

Figure 3. Horizontal component of electric displacement (D_x) of RF mode at 10 GHz

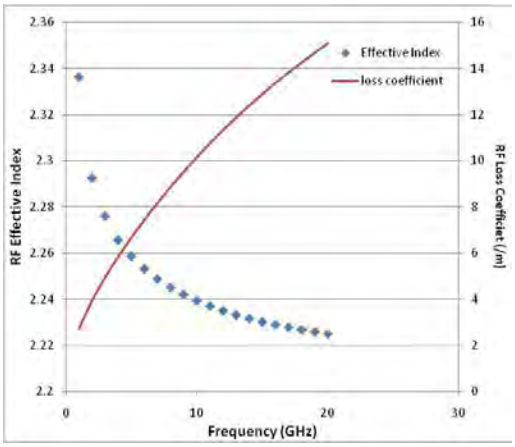

Figure 4. RF effective index and loss coefficient vs. frequency

The characteristic impedance, Z_0, of the coplanar waveguide is calculated from the computed current (I) and power (P) as:

$$Z_0 = 2\ P\ /\ |I|^2 \qquad (3)$$

The factor of 2 enters from the fact that the current is a peak value, while the power is a time-averaged quantity. Both P and I are calculated within Comsol by integration of their respective areal densities, the former over the entire domain, and the latter only over the center conductor. Since I is a complex quantity in time-harmonic models, the norm is used in equation (3). Figure 5 shows how the characteristic impedance varies with frequency.

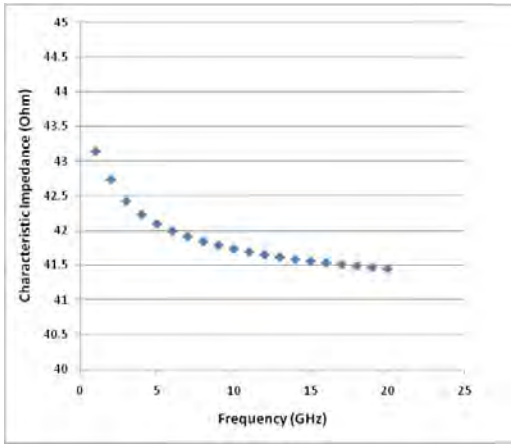

Figure 5. Characteristic impedance from equation (3) vs. frequency

3.2 Optical Mode Solutions, Velocity Matching and V_π

Since there are two channel waveguides, the mode solver will find two independent solutions, as shown in Figure 6. With no applied field, these two modes are degenerate, but when an electric field is applied, the effective indices split, as shown in Figure 7. (For a more accurate result, it is helpful to exaggerate the electro-optic coefficient by one or two orders of magnitude and scale the resulting Δn accordingly.)

To extract the value of V_π, it is necessary to know the applied voltage. Since the computed modes are not normalized, V must be extracted from the field. It can either be calculated directly by integrating the horizontal component of the electric field along a horizontal line between the electrodes, or indirectly from the previously calculated values of I and P as

$$|V|=2\ P/|I| \qquad (4)$$

In our experience the two methods produce essentially the same value.

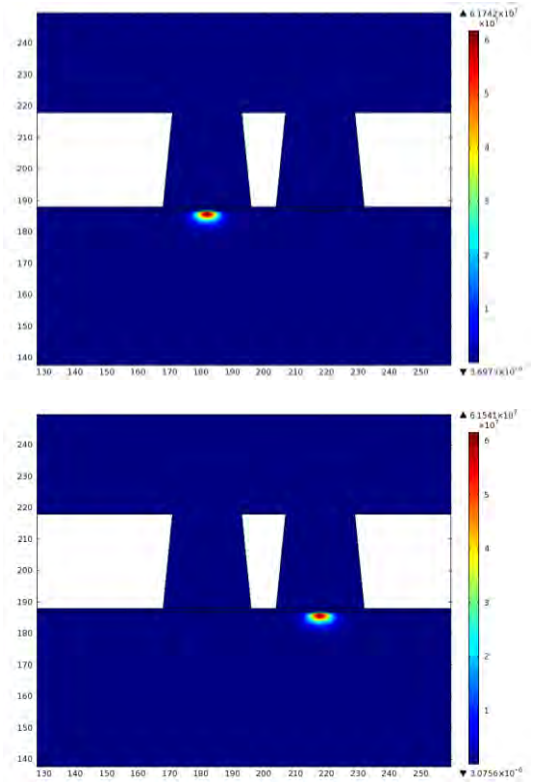

Figure 6. The optical modes in the left and right waveguides (norm of electric field)

The data of Figure 7 can be combined with the calculation of equation (4) to give the index change per volt, $\Delta n/V$. V_π is defined as the voltage at which the optical path difference is one-half wavelength. For a device length, L, it is given by:

$$V_\pi = \lambda/[2\ (\Delta n/V)\ L] \qquad (5)$$

It should be kept in mind that this value of V_π excludes electrode losses, and so is an underestimate, especially at higher frequencies.

Obviously, for a given electrode and waveguide design V_π can be reduced by

increasing the device length, L. However, increasing L also reduces the velocity-matching bandwidth, which is given by[1]:

$$f_c = c/[2\, n_m\, L\, (1-n_o/n_m)] \qquad (6)$$

where n_m and n_o are the effective indices of the RF and optical modes, respectively. Figure 8 shows V_π and f_c vs. L. (Since n_m and $\Delta n/V$ vary with frequency, the values at 20 GHz were used for this calculation.) Note that the optical waveguides in this example are not placed optimally. They could be moved closer to the center electrode, where the electric field is higher, to obtain a lower V_π.

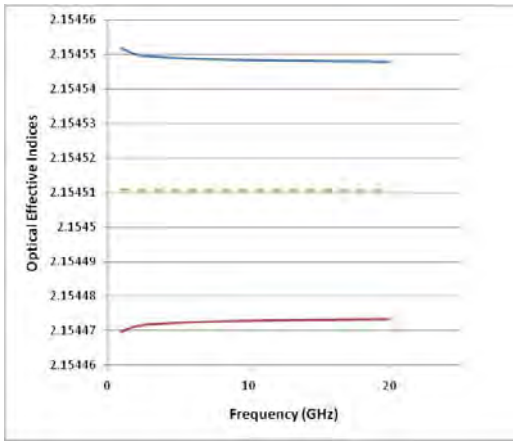

Figure 7. Effective indices of the optical modes in the left and right waveguides vs. frequency. The dashed line in the center is the zero-field value.

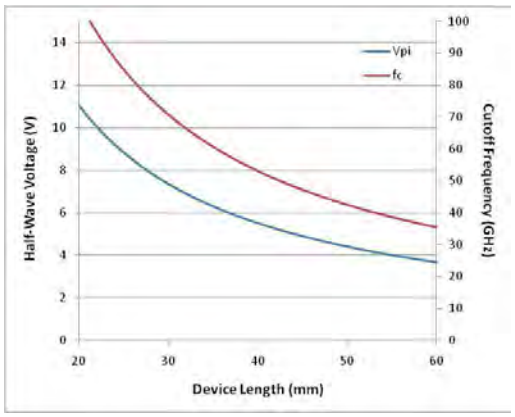

Figure 8. Half-wave voltage (neglecting electrode losses) and cutoff frequency vs. device length.

4. Combined Electrical-Optical Propagation Models

There are some important device considerations, such as the effect of RF loss on V_π, dependence of linearity on bias point and quasi-phase-matching, for which mode computations alone are insufficient. In these cases, a full 3D model that incorporates both RF and optical wave propagation would be helpful. However, because of the need for sub-wavelength meshing, 3D EM propagation over large distances at optical frequencies is impractical. The computational requirements can be reduced by using the paraxial approximation for the optical wave.[6] In this section we use a simplified, 2D example to demonstrate modeling of DC and RF electro-optic modulation in paraxial optical wave propagation.

4.1 DC-Optical Propagation Model

Figure 9 shows the geometry for a simplified, 2D, step-index model of a Mach-Zehnder interferometer (MZI). The optical propagation is done via the paraxial wave equation as in [6]. The voltage between the electrodes is applied using an electrostatics physics mode, and the change in refractive index is calculated via equation (1). In a more practical device model, the y-branches would use s-bends rather than straight lines. S-bends can be specified in Comsol via Bezier curves.

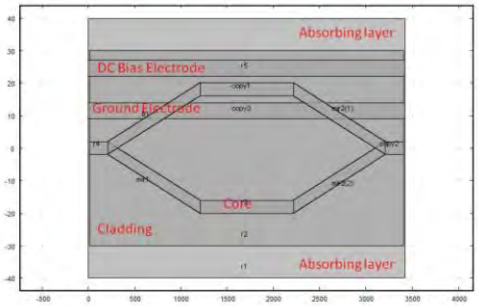

Figure 9. 2D geometry for optical propagation in MZI with DC modulation

The output of the model is shown in Figure 10 for applied voltages of 0 and 24 V. The quantity that is plotted is the square of the scalar field, which corresponds to optical intensity. For

0 V there is constructive interference and peak transmission, while for 24 V there is destructive interference and minimum transmission. Figure 11 shows the output power – calculated by integrating the intensity on a line across the output waveguide – vs. applied voltage, which exhibits the classic $1+\cos(\pi V/V_\pi)$ form. Since the active region of the device – the horizontal waveguide segment between the electrodes - is only 1 mm long, V_π is rather high at 24 V.

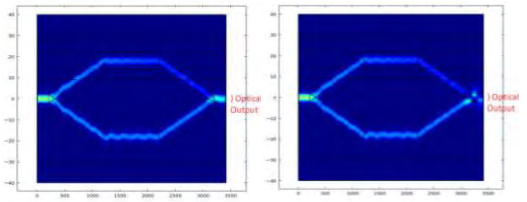

Figure 10. Paraxial optical propagation in a MZI with applied DC voltage of 0 V (left) and 24 V (right)

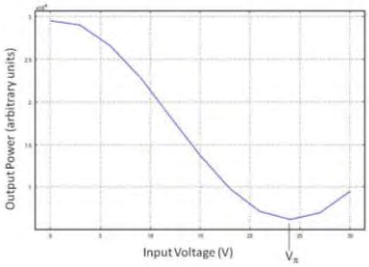

Figure 11. Output power vs. applied DC voltage in MZI

4.2 Time-Dependent RF-Optical Propagation Model

The geometry of Figure 9 can also be used for a combined RF-optical wave propagation model. The electrodes that were defined as equipotential surfaces in the DC model are treated as perfect electric conductors in the RF model. The space between the conductors represents the RF transmission domain, with the electric field profile specified at the input end and a scattering boundary condition at the output.

This setup is shown in Figure 12; the RF input and output are referred to as "ports" but they do not use the Port boundary condition, which applies only to time-harmonic models, whereas a time-dependent model is more appropriate in this case.

Since the frequency of the RF wave is extremely low on the optical time scale, the system is modeled as a time-dependent RF wave with a *static* optical wave computed at each time step. The electro-optic perturbation in refractive index is calculated from equation (1) at each time step based on the instantaneous RF E-field.

Figure 13 shows the input electric field and the optical output power vs. time over one period of the RF wave for small-signal (linear) modulation. In the first case (green curve), the MZI is biased at its half-power point, which gives maximum linearity. (In a real device biasing is achieved by applying a DC voltage. In this model it is done by adding a constant term to the refractive index of one arm of the interferometer.) In the second case, the MZI is biased at a point of zero slope (null), where the transmission is an even function of voltage. The result is frequency doubling, as can be seen in the figure.

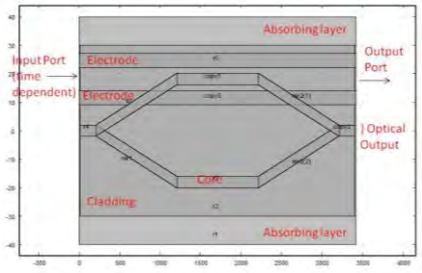

Figure 12. 2D geometry for optical propagation in MZI with RF modulation

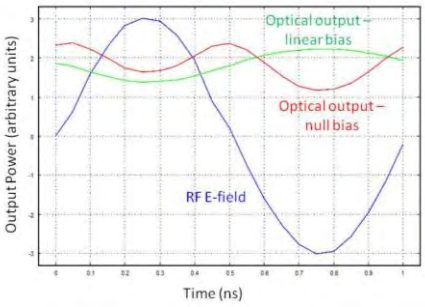

Figure 13. Input RF field and optical output power for small-signal modulation with MZI at linear (green) and nonlinear (red) bias points. In the latter case, frequency doubling occurs.

5. Conclusions

We have demonstrated the use of Comsol Multiphysics in an integrated approach to modeling of electro-optic devices. In combined RF-optical mode solving, Comsol provides the flexibility for realistic treatment of material properties and waveguide profiles.

We have demonstrated how a combined RF-optical wave propagation model can be constructed via a simplified 2D example. Construction of realistic 3D models to study more complex phenomena such as the impact of electrode loss on V_π and quasi-phase-matched structures is possible, given greater computing resources.

6. References

1. R.C. Alferness, S.K. Korotky and E.A.J. Marcatili, "Velocity-Matching Techniques for Integrated Optic Traveling Wave Switch/Modulators," *IEEE J. Quantum Electronics* **QE-20**, 301-9 (1984)
2. A. Passaro, M.A.R. Franco, N.M. Abe and F. Sircilli, "The Effect of the Proton-Concentration-to-Refractive-Index Models on the Propagation Properties of APE Waveguides," *J. Lightwave Tech.* **20**, 1573-7 (2002)
3. P.E. Powers, *Fundamentals of Nonlinear Optics*, pp. 70-74, CRC Press, Boca Raton (2011)
4. J.M. Hammer, "Modulation and Switching of Light in Dielectric Waveguides," in T. Tamir (ed.), *Integrated Optics*, p. 149, Springer-Verlag, Berlin (1979)
5. R-Y Yang, Y-K Su, M-H Weng, C-Y Hung and H-W Wu, "Characteristics of Coplanar Waveguide on Lithium Niobate Crystals as a Microwave Substrate," *J. Appl. Phys.* **101**, 014101 (2007)
6. J.E. Toney, "Implementation of a Paraxial Optical Propagation Method for Large Photonic Devices," *Comsol 2009*, Newton, MA (October 2009)

7. Acknowledgements

I offer thanks to my colleagues, Dr. Sri Sriram and Dr. Vincent Stenger, for helpful discussions on the practical aspects of electro-optic modulator design.